Research Article

Chemical Review and Letters
journal homepage: www.chemrevlett.com
ISSN (online): 2645-4947 (print) 2676-7279

Procarbazine adsorption on the surface of single walled carbon nanotube: DFT studies

Mohammad Reza Jalali Sarvestani[a], Roya Ahmadi[b,*], Behnam Farhang Rik [c]

[a] *Young Researchers and Elite Clube, Yadegar-e-Imam Khomeini (RAH) Shahre-rey Branch, Islamic Azad University, Tehran, Iran*
[b]*Department of Chemistry, Yadegar-e-Imam Khomeini (RAH) Shahre-rey Branch, Islamic Azad University, Tehran, Iran*
[c]*Department of Inorganic Chemistry, Faculty of Chemistry, Tehran North Branch, Islamic Azad University, Tehran, Iran*

ARTICLE INFO

Article history:
Received 31 May 2020
Received in revised form 10 July 2020
Accepted 14 July 2020
Available online 22 July 2020

Keywords:
Procarbazine
DFT
Carbon nanotube
Adsorption

ABSTRACT

In this research, the performance of single-walled carbon nanotube (SWCN) as a sensor and nanocarrier for procarbazine (PC) was investigated by infra-red (IR), natural bond orbital (NBO), frontier molecular orbital (FMO) computations. All of the computations were done using the density functional theory method in the B3LYP/6-31G (d) level of theory The calculated negative values of adsorption energy, enthalpy changes, Gibbs free energy changes showed the PC interaction with SWCN is exothermic, spontaneous and experimentally possible. The increasing of specific heat capacity (C_V) of SWCN after adsorption of PC showed the thermal conductivity improved during the interaction process and this nanostructure is an excellent sensing material for the detection of PC. The NBO results demonstrate in all of the evaluated conformers a chemical bond with SP^3 hybridization is formed between the medicine and SWCN. The great values of thermodynamic constants showed the adsorption process is irreversible and SWCN is not a suitable nanocarrier for delivery of PC. The density of states (DOS) spectrums showed the bandgap of SWCN decreased sharply after the adsorption of PC and this nanomaterial can be used as a sensor for electrochemical detection of PC.

1. Introduction

Procarbazine (PC) which its optimized structure is given in the Figure 1, is a cytotoxic chemotherapeutic medicine that is prescribed orally for the treatment of lymphomas and brain tumors. PC was approved for the first time in 1969 and it is on the WHO list of essential medicines [1-5]. PC has high toxicity and severe adverse effects like bloody vomit, fever, unusual bleeding or bruising, hallucinations, fainting, nervousness, depression, lethargy and liver malfunction. In this regard, finding a new nanocarrier and detection method for PC is very important [6-8]. On the other hand, single-walled carbon nanotube (SWCN) is an allotrope of carbon. This nanostructure consists of a cylindrical graphene sheet with a length of about a few microns and a diameter of 0.4 to 2 nanometers (Figure 1). SWCN has unique features, including high surface-to-volume ratio, high thermal conductivity, medium electrical conductivity and high tensile strength [9-13]. And these outstanding properties have led to the application of this nanomaterial in various fields such as biosensors and sensors, removal of environmental contaminants, drug delivery, super-capacitors and the development of new extraction methods [14-17]. In this regard, it was decided to investigate the performance of SWCN as a novel nanocarrier and sensor for drug delivery and determination of PC for the first time by IR, NBO and FMO computations.

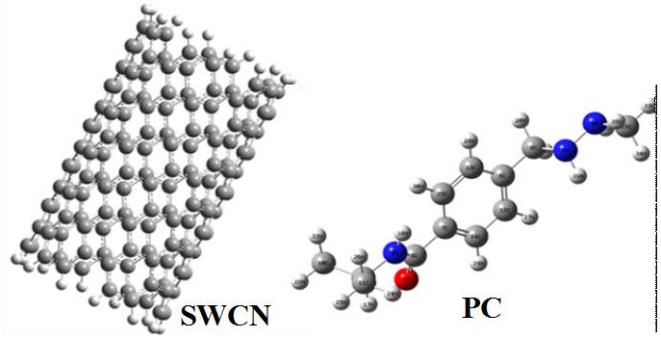

Figure 1. Optimized structures of PC and SWCN

2. Structural and NBO Analysis

The initial and optimized structures of PC-SWCN complexes are provided in Figure 2. As it is clear, the PC interaction with the nanostructure was investigated at two different modes. In A-Conformer, the PC molecule was inserted in a parallel form on the surface of carbon nanotube but in B-conformer, the PC approaches the adsorbent surface towards its methyl group. After the geometrical optimizations were performed on the structures the structures of PC and SWCN deformed on some interacting sites which can be due to the formation of some chemical bonds between them. In this respect, for obtaining more information about the adsorption mechanism the adsorption energy values of both conformers were calculated and NBO computations were also done on them and the results are tabulated in Table 1. As can be seen, the adsorption energy values of A and B conformers are -291.909 and -310.288 kJ/mol respectively, indicating the adsorption process is experimentally possible and B-Conformer is more energetically stable than A-Conformer [18-120].

The NBO results showed in both configurations a covalent (two electrons containing) bond with SP^3 hybridization and bond order of 1 is created between the PC and SWCN. Therefore, PC interaction with the nanotube is chemisorption. Hence, it can be concluded that SWCN cannot be a suitable nanocarrier for drug delivery of PC. The dipole moment of the studied structures was also calculated. As can be seen from Table 1, the PC-SWCN complexes have higher dipole moment values than pure PC which implies the solubility and bioavailability of PC improved after its adsorption on the surface of SWCN. It should be noted that according to the performed IR computations no negative vibrational frequency was observed for the studied structures which indicate all of the investigated structures are a true local minimum [21-24].

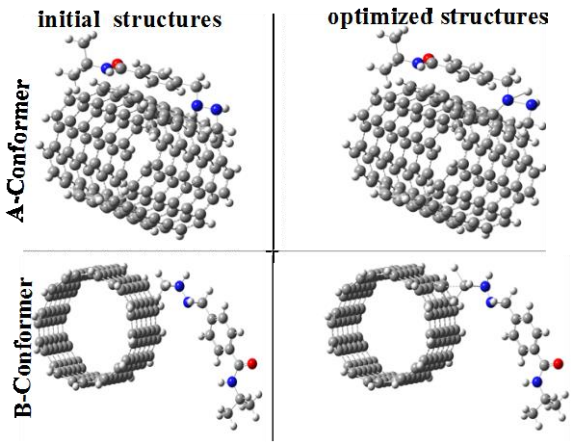

Figure 2. The initial and optimized structures of PC-SWCN complexes

Table 1. The calculated structural and NBO parameters of PC, SWCN and their complexes

	PC	SWCN	A-Conformer	B-Conformer
	---	---	N3-C	C10-C
Dipole moment(Deby)	3.48	0	7.88	9.91
The lowest frequency (cm-1)	33.464	89.411	23.246	37.891
Adsorption energy (kJ/mol)	---	---	-291.909	-310.288
Total electronic energy (a.u)	-1123.631	-1353.143	-2476.924	-2476.931
Bond energy (a.u.)	---	---	-0.382	-0.41
Hybridization	---	---	Sp2.98	Sp3.01
Occupancy	---	---	1.98	1.96
Bond order	---	---	1	1
Bond length (Å)	---	---	1.72	1.61

3. Thermodynamic parameters

The calculated adsorption enthalpy changes (ΔHad) and specific heat capacity (CV) are reported in Table 2. As the provided data in Table 2 reveal clearly, the PC interaction with the nanotube is exothermic because of the obtained highly negative ΔHad values. Besides, the C_V of the nanostructure and the PC increases sharply when PC adsorbs on the surface of SWCN which indicates the thermal conductivity enhances remarkably in the adsorption process. Therefore, it can be concluded that SWCN is an appropriate sensing material for the construction of a thermal sensor for the detection of PC. In thermal sensors, the analyte should have a highly exothermic or endothermic interaction with the immobilized recognition element on the sensor surface (here SWCN) then the carried out variation in the temperature of the sensor microenvironment will be measured by a sensitive thermistor and it will be used as a signal for detection of the analyte [25].

Table 2. The calculated values of adsorption enthalpy changes and specific heat capacity in temperature range of 298-398 K.

Temperature (K)	ΔH_{ad} (kJ/mol)		C_V (J/mol. K)			
	A-Conformer	B-Conformer	A-Conformer	B-Conformer	PC	SWCN
298	-527.441	-545.819	499.890	530.266	389.277	178.175
308	-526.990	-545.368	517.488	547.472	400.287	184.106
318	-526.593	-544.972	535.133	564.713	411.339	190.041
328	-526.245	-544.623	552.802	581.966	422.417	195.967
338	-525.949	-544.327	570.469	599.206	433.509	201.873
348	-525.651	-544.029	588.110	616.410	444.600	207.746
358	-525.374	-543.753	605.702	633.554	455.675	213.577
368	-525.049	-543.427	623.221	650.618	466.720	219.356
378	-524.685	-543.064	640.647	667.580	477.722	225.077
388	-524.310	-542.689	657.958	684.421	488.666	230.730
398	-523.925	-542.303	675.134	701.123	499.542	236.311

The calculated values of Gibbs free energy variations (ΔG_{ad}) and thermodynamic equilibrium constants (K_{th}) are presented in Table 3. As it is obvious, the PC adsorption process is spontaneous and irreversible because of the highly negative values of ΔGad and great values of Kth. The effect of temperature on both parameters was also investigated. As the results showed clearly by increasing temperature the ΔG_{ad} and K_{th} experience a tangible increase and decrease which indicates the adsorption process is more favorable in lower temperatures [26-28].

Table 3. The calculated values of Gibbs free energy changes and thermodynamic equilibrium constants in the temperature range of 298-398 K.

Temperature (K)	ΔG_{ad} (kJ/mol)		K_{th}	
	A-Conformer	B-Conformer	A-Conformer	B-Conformer
298	-468.878	-487.257	$1.408\times10^{+82}$	$2.336\times10^{+85}$
308	-466.822	-485.200	$1.361\times10^{+79}$	$1.776\times10^{+82}$
318	-464.806	-483.184	$2.069\times10^{+76}$	$2.154\times10^{+79}$
328	-462.809	-481.188	$4.702\times10^{+73}$	$3.961\times10^{+76}$
338	-460.891	-479.270	$1.575\times10^{+71}$	$1.087\times10^{+74}$
348	-458.946	-477.324	$7.250\times10^{+68}$	$4.148\times10^{+71}$
358	-456.989	-475.368	$4.491\times10^{+66}$	$2.152\times10^{+69}$
368	-454.908	-473.287	$3.520\times10^{+64}$	$1.427\times10^{+67}$
378	-452.708	-471.086	$3.433\times10^{+62}$	$1.187\times10^{+65}$
388	-450.372	-468.750	$4.076\times10^{+60}$	$1.212\times10^{+63}$
398	-447.907	-466.286	$5.815\times10^{+58}$	$1.499\times10^{+61}$

4. FMO Analysis

The electrical conductance of a compound has an inverse relationship with its bandgap (E_g) which is defined as the energy difference between the highest occupied molecular orbital (HOMO) and the lowest unoccupied molecular orbital (LUMO). In order to evaluate the performance of SWCN as an electrochemical sensing material for detection of PC, the DOS spectrum of each structure was computed and the obtained results is presented in Figure 3. As can be observed, the bandgap of the nanostructure is 6.896 eV but when PC adsorbs on its surface the E_g decreased to 5.218 and 6.304 eV in A and B conformers respectively. This phenomenon indicates the electrical conductivity of SWCN improved significantly in the PC adsorption process. Hence, it can be deduced that this nanomaterial is an excellent electroactive sensing material for the development of new electrochemical sensors for the determination of PC [29]. Other important frontier molecular orbital parameters like chemical hardness (η), chemical potential (μ), electrophilicity (ω) and maximum charge capacity (ΔN_{max}) were also calculated and the results are given in Table 4. The chemical hardness and chemical potential have an obvious relationship with the reactivity of a material. Indeed, the molecules with lower amounts of η and higher values of μ are more reactive because the important electron transmissions that are necessary for the implementation of a chemical reaction is done in them easier [30-32]. As can be seen, when PC interacts with the SWCN, η and μ decline and increase respectively which indicates PC-SWCN complexes are more reactive than pure PC. ω and ΔN_{max} are good parameters for estimating the affinity of a molecule towards an electron. In other words, the compounds with higher values of ω and lower amounts of ΔN_{max} have more tendency to absorb electron. As it is clear from Table 4, the electrophilicity of PC and maximum transferred charge capacity experience a meaningful increase and decrease respectively which implies PC complexes with carbon nanotube are more electrophile in comparison to pure PC without the adsorbent [33, 34].

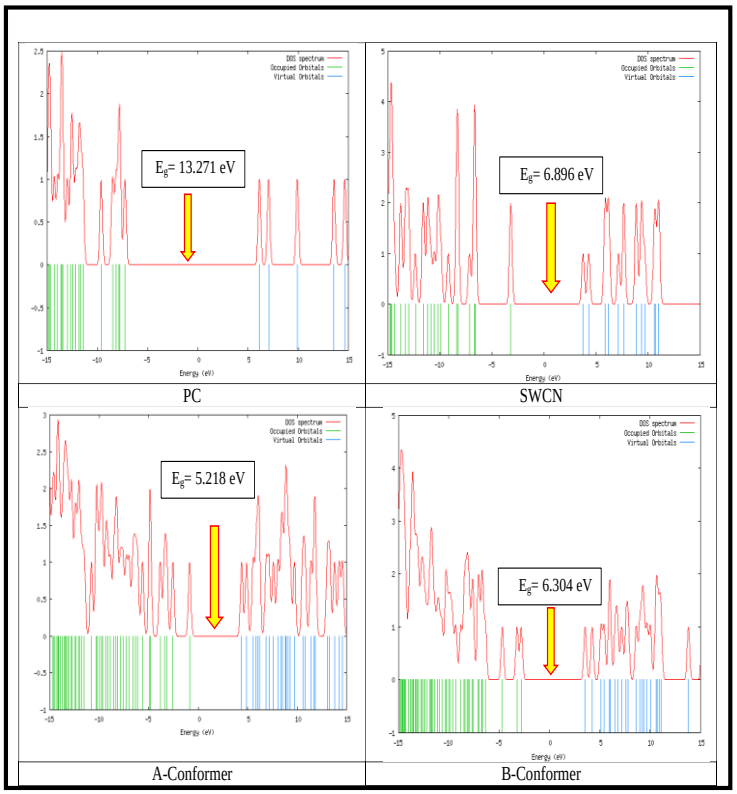

Figure 3. The DOS spectrums of PC, SWCN and their complexes

Table 4. The calculated frontier molecular orbital parameters for PC, SWCN and their complexes

	E_H (eV)	E_L (eV)	E_g (eV)	η (eV)	μ (eV)	ω (eV)	ΔN_{max} (eV)
PC	-7.185	6.087	13.271	6.636	-0.549	0.023	0.083
SWCN	-3.186	3.709	6.896	3.448	0.261	0.010	-0.076
A-Conformer	-0.851	4.367	5.218	2.609	1.758	0.592	-0.674
B-Conformer	-2.795	3.509	6.304	3.152	0.357	0.020	-0.113

5. Computational Details

The structures of SWCN, PC and their complexes at two different configurations were designed by Nanotube modeler 1.3.0.3 and GuassView 6 softwares [21, 22]. After the geometrical optimization of structures, IR, NBO and FMO computations were implemented on them using the density functional theory method in the B3LYP/6-31G (d) level of theory [23]. This level of theory was selected because in former reports about nanomaterials its results bear a lot of resemblance with the experimental findings. GuassSum 3.0 software was used for obtaining the density of states (DOS) spectrums [24]. All of the computations were done in the aqueous phase in the temperature range of 298-398 at 10˚ intervals.

The studied processes were as follows:

PC + SWCN ⟶ PC-SWCN (1)

The values of adsorption energy values (Ead) and thermodynamic parameters including adsorption enthalpy changes (ΔH_{ad}), Gibbs free energy changes (ΔG_{ad}) thermodynamic equilibrium constants (K_{th}) and entropy changes (ΔS_{ad}) were calculated by Equations 2-5 respectively.

$$E_{ad} = \left(E_{(\text{PC-SWCN})} - \left(E_{(\text{PC})} + E_{(SWCN)} + E_{(BSSE)}\right)\right) \quad (2)$$

$$\Delta H_{ad} = \left(H_{(\text{PC-SWCN})} - \left(H_{(\text{PC})} + H_{(SWCN)}\right)\right) \quad (3)$$

$$\Delta G_{ad} = \left(G_{(\text{PC-SWCN})} - \left(G_{(\text{PC})} + G_{(SWCN)}\right)\right) \quad (4)$$

$$K_{th} = \exp\left(-\frac{\Delta G_{ad}}{RT}\right) \quad (5)$$

In the referred equations, E is the total electronic energy of each structure, E_{BSSE} denotes the basis set superposition correction, H stands for the enthalpy of the evaluated materials. The G denotes Gibbs free energy of the studied structures. R is the ideal gas constants and T denotes the temperature [18, 19].
Frontier molecular orbital parameters including bandgap (Eg), chemical hardness (η), chemical potential (μ), electrophilicity (ω) and the maximum charge capacity (ΔNmax) were calculated by equations 6-10 [10].

$$\text{Eg} = E_{LUMO} - E_{HOMO} \quad (6)$$

$$\eta = \left(E_{LUMO} - E_{HOMO}\right)/_2 \quad (7)$$

$$\mu = \left(E_{LUMO} + E_{HOMO}\right)/_2 \quad (8)$$

$$\omega = \mu^2/_{2\eta} \quad (9)$$

$$\Delta N_{max} = -\mu/_{\eta} \quad (10)$$

E_{LUMO} and E_{HOMO} in equations 6 to 11 are the energy of the lowest unoccupied molecular orbital and the energy of the highest occupied molecular orbital respectively [14].

4. Conclusion

Developing a new effective nanocarrier and sensor for delivery and detection of PC is of great importance. On the other hand, SWCN has special properties that make it a suitable nanocarrier and sensor for various pharmaceutical compounds. İn this respect, the performance of SWCN as nanocarrier and a thermal/electrochemical sensor for detection of procarbazine was evaluated in this research by DFT calculations. Owing to the fact that the NBO results and thermodynamic constants showed the PC interaction with SWCN is chemisorption and irreversible. Hence, SWCN is not an appropriate nanocarrier for drug delivery of PC. But the values of specific heat capacity and bandgap showed the electrical and thermal conductivity of SWCN is a suitable sensing material for the construction of new thermal and electrochemical sensors for the detection of PC.

Acknowledgements

The authors appreciate the young researchers and elite club of Islamic Azad University of Yadegar-e-Imam Khomeini (RAH) Shahre-rey branch for supporting this project.

References

[1] X. He, T. T. Batchelor, S.Grossman, J. G. Supkoafor, Determination of procarbazine in human plasma by liquid chromatography with electrospray ionization mass spectrometry. J. Chromatogr. B., 799 (2004) 281-291.
[2] R. M. Gorsen, A. J. Weiss, R. W. Manthei, Analysis of Procarbazine and Metabolites by Gas Chromatography-Mass Spectrometry. J. Chromatogr., 221 (1980) 309-318.
[3] P. Rainer, B. Frank, R. Ralf, M. Michael, Plasma kinetics of procarbazine and azo-procarbazine in humans. Anti-Cancer Drugs., 17 (2006) 75-80.
[4] D. F. Lehmann, T. E. Hurteau, N. Newman, T. E. Coyle, Anticonvulsant usage is associated with an increased risk of procarbazine hypersensitivity reactions in patients with brain tumors. Clin. Pharmacol. Ther., 62 (1997) 225-229.
[5] S. Clifford Schold, T. P. Brent, E. Hofe, H. S. Friedman, S. Mitra, D. D. Bigner, J. A. Swenberg, D.V.M., P. Kleihues, M.D. 1O6-Alkylguanine-DNA alkyltransferase and sensitivity to procarbazine in human brain-tumor xenografts. Superlattices Microstruct., 70 (1989) 573-577.
[6] B. Farhang Rik, R. Ranjineh Khojasteh, R. Ahmadi, M. Karegar Razi, Evaluation of C60 nano-structure performance as nano-carriers of procarbazine anti-cancer drug using density functional theory methods. Iran. Chem. Commun., 7 (2019) 405-414.
[7] A. Taherpour, A. Hassani Daramroudi, R. Kariminya, Theoretical study of diffusion flow of anticancer medicines through single-wall armchair (10, 10) carbon nanotube. J Control Release., 1 (2019) 56-61.
[8] F. Simon, H. Peterlik, R. Pfeiffer, J. Bernardi, H. Kuzmany, Fullerene release from the inside of carbon nanotubes: A possible route toward drug delivery. Chem. Phys. Lett., 445 (2007) 288-292.
[9] M.Gallo, A. Favila, D. G. Mitnik, DFT studies of functionalized carbon nanotubes and fullerenes as nanovectors for drug delivery of antitubercular compounds. Chem. Phys. Lett., 447 (2007) 105-109.
[10] R. Ahmadi, M. Pirahan-Foroush, Ab initio studies of fullerene effect on chemical properties of naphazoline drop. Ann. Mil. Health. Sci. Res., 12 (2014) 86-90.
[11] J. Shi, Y. Liu, L.Wang, J. Gao, J. Zhang, X.Yu, Ma R. R. Liu , Z. Zhang, A tumoral acidic pH-responsive drug deliv, ery system based on a novel photosensitizer (fullerene) for in vitro and in vivo chemo-photodynamic therapy. Acta. Biomater., 10 (2014) 1280-1291.
[12] M. K. Hazrati, N. L. Hadipour, Adsorption behavior of 5-fluorouracil on pristine, B-, Si-, and Al-doped C_{60} fullerenes: A first-principles study. Phys. Lett., 380 (2016), 937-941.
[13] Ö.Alver, M.Bilge, N.Atar, C.Parlak, M. Şenyel, Interaction mechanisms and structural properties of MC19 (M=Si and Al)

fullerenes with chlorophenylpiperazine isomers. J. Mol. Liq., 231(2017) 202-205.
[14] R. Ahmadi, T.Boroushaki, M. Ezzati, Study on effect of addition of nicotine on nanofullerene structure C60 as a medicine nanocarrier. Orient. J. Chem., 28 (2012) 773-9.
[15] J.Lenik, C. Wardak, Characteristic of a new sensor for indomethacin determination. Procedia. Eng., 47 (2012) 144-147.
[16] T. Baciu, I. Botello, F. Borrull, M. Calull, C. Aguilar, Capillary electrophoresis and related techniques in the determinationof drugs of abuse and their metabolites. Trends Anal. Chem, 74(2015) 89-108.
[17] M. R. Moeller, S. Steinmeyer, T.Kraemer, Determination of drugs of abuse in blood. J. Chromatogr. B, 713(1998) 91-109.
[18] K. Vytras, The use of ion-selective electrodes in the determination of drug substances. J. Pharm. Biomed. Anal., 7(2002) 789-812.
[19] M. Eslami, M. Moradi, R. Moradi, Physica. E. LowDimens. Syst. Nanostruct, 87(2017) 186-191.
[20] S.Bashiri, E.Vessally, A. Bekhradnia, A. Hosseinian, L. Edjlali, Utility of extrinsic [60] fullerenes as work function type sensors for amphetamine drug detection: DFT studies. Vacuum., 136 (2016) 156-162.
[21] nanotube Modeler J. Crystal. Soft., 2014 software.
[22] GaussView, Version 6.1, R. Dennington, T. A. Keith, J. M. Millam, Semichem Inc., Shawnee Mission, KS, 2016.
[23] Gaussian 16, Revision C.01, M. J. Frisch, G. W. Trucks, H. B. Schlegel, G. E. Scuseria, M. A. Robb, J. R. Cheeseman, G. Scalmani, V. Barone, G. A. Petersson, H. Nakatsuji, X. Li, M. Caricato, A. V. Marenich, J. Bloino, B. G. Janesko, R. Gomperts, B. Mennucci, H. P. Hratchian, J. V. Ortiz, A. F. Izmaylov, J. L. Sonnenberg, D. Williams-Young, F. Ding, F. Lipparini, F. Egidi, J. Goings, B. Peng, A. Petrone, T. Henderson, D. Ranasinghe, V. G. Zakrzewski, J. Gao, N. Rega, G. Zheng, W. Liang, M. Hada, M. Ehara, K. Toyota, R. Fukuda, J. Hasegawa, M. Ishida, T. Nakajima, Y. Honda, O. Kitao, H. Nakai, T. Vreven, K. Throssell, J. A. Montgomery, Jr., J. E. Peralta, F. Ogliaro, M. J. Bearpark, J. J. Heyd, E. N. Brothers, K. N. Kudin, V. N. Staroverov, T. A. Keith, R. Kobayashi, J. Normand, K. Raghavachari, A. P. Rendell, J. C. Burant, S. S. Iyengar, J. Tomasi, M. Cossi, J. M. Millam, M. Klene, C. Adamo, R. Cammi, J. W. Ochterski, R. L. Martin, K. Morokuma, O. Farkas, J. B. Foresman, and D. J. Fox, Gaussian, Inc., Wallingford CT, 2016.
[24] N. M. O'Boyle, A. L. Tenderholt, K. M. Langner, A Library for Package-Independent Computational Chemistry Algorithms. J. Comp. Chem., 29 (2008) 839-845.
[25] R. Ahmadi, M. R. Jalali Sarvestani, Adsorption of Tetranitrocarbazole on the Surface of Six Carbon-Based Nanostructures: A Density Functional Theory Investigation. Phys. Chem. B., 14 (2020) 198-208.
[26] M. R. Jalali Sarvestani, R. Ahmadi, Adsorption of TNT on the surface of pristine and N-doped carbon nanocone: A theoretical study. Asian J. Nanosci. Mater., 3 (2020) 103-114.
[27] M. R. Jalali Sarvestani, M. Gholizadeh Arashti, B. Mohasseb, Quetiapine Adsorption on the Surface of Boron Nitride Nanocage (B12N12): A Computational Study. Int. J. New. Chem., 7 (2020) 87-100.
[28] M. R. Jalali Sarvestani, R. Ahmadi, Investigating the Complexation of a recently synthesized phenothiazine with Different Metals by Density Functional Theory. Int. J. New. Chem., 4 (2017) 101-110.
[29] M. R. Jalali Sarvestani, R. Ahmadi, Adsorption of Tetryl on the Surface of B12N12: A Comprehensive DFT Study. Chem. Methodol., 4 (2020) 40-54.
[30] S. Majedi, F. Behmagham, M. Vakili, Theoretical view on interaction between boron nitride nanostructures and some drugs. J. Chem. Lett., 1 (2020) 19-24.
[31] H. G. Rauf, S. Majedi, E. A. Mahmood, M. Sofi, Adsorption behavior of the Al- and Ga-doped B12N12 nanocages on COn (n=1, 2) and HnX (n=2, 3 and X=O, N): A comparative study. Chem. Rev. Lett., 2 (2019) 140-150.
[32] R. A. Mohamed, U. Adamu, U. Sani, S. A. Gideon, A. Yakub, Thermodynamics and kinetics of 1-fluoro-2-methoxypropane vs Bromine monoxide radical (BrO): A computational view. Chem. Rev. Lett., 2 (2019) 107-117.
[33] S. Majedi, H. G. Rauf, M. Boustanbakhsh, DFT study on sensing possibility of the pristine and Al- and Ga-embeded B12N12 nanostructures toward hydrazine and hydrogen peroxide and their analogues. Chem. Rev. Lett. 2 (2019) 176-186.
[34] R. Moladoust, Sensing performance of boron nitride nanosheets to a toxic gas cyanogen chloride: Computational exploring. Chem. Rev. Lett., 2 (2019) 151-156.